

## Ramsey Fringes in Germanium Doped with Arsenic Donors

R. Kh. Zhukavin<sup>a, \*</sup>, P. A. Bushuikin<sup>a</sup>, V. D. Kukotenko<sup>b</sup>, Yu. Yu. Choporova<sup>b</sup>, N. Deßmann<sup>d</sup>,  
K. A. Kovalevsky<sup>a</sup>, V. V. Tsyplenkov<sup>a</sup>, N. D. Osintseva<sup>b</sup>, V. V. Gerasimov<sup>b, c</sup>, D. V. Shengurov<sup>a</sup>,  
B. A. Knyazev<sup>c</sup>, N. V. Abrosimov<sup>e</sup>, and V. N. Shastin<sup>a</sup>

<sup>a</sup> Institute for Physics of Microstructures, Institute of Applied Physics, Russian Academy of Sciences,  
Nizhny Novgorod, 603950 Russia

<sup>b</sup> Budker Institute of Nuclear Physics, Siberian Branch, Russian Academy of Sciences, Novosibirsk, 630090 Russia

<sup>c</sup> Novosibirsk State University, Novosibirsk, 630090 Russia

<sup>d</sup> FELIX Laboratory, Radboud University, Nijmegen, 6525 ED The Netherland

<sup>e</sup> Leibniz-Institut für Kristallzüchtung, Berlin, 12489 Germany

\*e-mail: zhur@ipmras.ru

Received December 5, 2022; revised December 23, 2022; accepted February 27, 2023

**Abstract**—The results of observation of Ramsey oscillations in germanium doped with arsenic donors detected by photothermal ionization of Coulomb centers are presented. To excite quantum coherent superpositions of the states at the transition  $1s(A_1)–2p_0$  the Novosibirsk free electron laser radiation was used. The results are analyzed using a theoretical model using several key parameters of the experiment.

**Keywords:** germanium, donor, Ramsey fringes, coherence, terahertz radiation

**DOI:** 10.3103/S1062873823702039

### INTRODUCTION

Currently, intensive research is underway on the most suitable objects for creating new nanoelectronic devices based on the fundamental quantum behavior of constituent elements. In particular, one can note the search for a platform for reliable and technologically advanced approach for implementation of quantum memory, encryption systems, quantum metrology, quantum computers, and so on. To date, the element base has not been finally created, which would have good scalability and a high degree of control over each element of the system separately. Among the promising areas of research, elementary semiconductors are distinguished by the fact that they have one of the most technologically mastered media, such as silicon, germanium, and diamond, for which record degrees of chemical and isotopic purity have been obtained [1, 2], as well as high-quality single crystals and various structures for the purposes of nanoelectronics, including technologies with atomic resolution [3].

The possibility of using one or another physical system for recording, storing, and reading the information is determined primarily by the times of longitudinal  $T_1$  and transverse  $T_2$  relaxation. In the case of using the semiconductors, the introduction of zero-dimensional objects with a discrete spectrum is assumed, which, in the case of resonant excitation, makes it possible to implement a two-level model. Such objects include quantum dots [4] and various

impurity centers (donors, acceptors, and complexes formed with their participation). As a rule, for all these cases, we are talking about the use of magnetic dipole transitions with small matrix elements, which makes it possible to obtain sufficiently large population relaxation times [5, 6]. When using transitions between states that differ only by spin, as in the case of two components of the ground state of a donor in a magnetic field, in experiments, as a rule, the magnitude of the magnetic field corresponds to transition frequencies much lower than 1 THz, which requires the use of temperatures below the temperature of liquid helium. In this regard, it becomes necessary to search for conditions, systems, and methods under which it is possible to use higher temperatures, and, consequently, higher frequencies to control the states of a two-level system. Very encouraging are the results obtained for donors in silicon [7] and NV centers in diamond [8], where near-IR radiation was used. In the case of germanium, work is carried out using quantum dots, but donors or acceptors are studied much less frequently, which is associated with a smaller scale of binding energies of hydrogen-like impurities and excitons. Nevertheless, donors in germanium have characteristics that make it possible to hope for their use in the further development of existing technologies. Due to the rather small effective mass ( $m_e/m_0 \sim 0.08$ ) and large permittivity ( $\epsilon \sim 16$ ), the radii of the ground state of the donor turn out to be much larger compared to the

case of silicon, which reduces the requirements for creating planar arrays with control gates in schemes having the architecture Kane [9]. When using optical control methods, an important role is played by the value of the matrix elements of transitions between localized states [10], which also favorably distinguishes germanium against silicon and diamond. The obtained experimental data reveal relatively long (nanosecond scale) relaxation times for the selected donor transitions in germanium [11]. An additional factor is the possibility of obtaining isotopically pure (or enriched) germanium and the possibility of doping it by nuclear transmutation, which makes it possible to create a uniform distribution of impurity centers [12]. In the case of using hydrogen-like donors in germanium to control intracenter dipole transitions, radiation sources in the terahertz range are required, which have recently been developed, including those with a pulsed structure and a narrow line, such as quantum-cascade lasers [13] or lasers based on  $p$ -Ge [14]. Until recently, the possibility of creating coherent superpositions of the states of a Coulomb center has been studied in sufficient detail with respect to donors in silicon by quantum optics methods, such as photon echo and Ramsey fringes [15]. Relatively recently, it was shown that the lifetimes of donor states in germanium exceed those for silicon, which gave hope for the possibility of using existing technical means to study such systems by quantum optics methods [16]. Subsequently, the first short report on the detection of Ramsey fringes for arsenic in germanium was published [17].

This publication is aimed at a more detailed analysis of experimental data based on a theoretical approach that considers the relaxation of the population and coherence in the system, which makes it possible to obtain a more correct description of the signal shape.

## EFFECT DESCRIPTION

As is known, for Ramsey interferometry two pulses are usually used [18, 17]. The first radiation pulse at a frequency close to the intracenter transition frequency ( $\omega \sim \omega_0$ ) excites a coherent superposition of impurity states. It is optimal to use  $\pi/2$  pulse (Fig. 1a), i.e. when the system is excited at the equator of the Bloch sphere (an impurity atom in this state has the maximum possible dipole moment for a given transition). The system continues to be in this state even after the end of the action of the excitation pulse. The second  $\pi/2$  pulse following with some time delay in the case of exact resonance ( $\omega = \omega_0$ ) transfers the system either to the upper state of the excited transition (the pole on the Bloch sphere), if the radiation in the second pulse is in phase with the excited dipole ( $\varphi = 0$ ), or returns to the initial lower state of the transition, if the second pulse arrives in antiphase ( $\varphi = \pi$ ). In the case of an arbitrary value of the phase difference  $\varphi$ , the system

remains in a certain superposition of impurity states with a nonzero value of the dipole moment (the dipole moment of an impurity is nonzero only in the superposition of states). Thus, the phase adjustment of the quantum state of the impurity atom is carried out. In this case, the phase difference in the experiment is controlled by the delay time  $\tau$  of the second radiation pulse relative to the first one (Fig. 1). The detection of the final state of the system in this work was carried out by measuring the photocurrent due to the thermal ejection of carriers into the conduction band from the upper state of the excited transition. Thus, the value of the measured photocurrent depends on the final state of the atom after the action of a sequence of two radiation pulses, which in turn depends on the delay time between pulses. The resulting dependence is an oscillating function with an oscillation period corresponding to the frequency of the excited transition. This effect is strongly dependent on the detuning value  $\Delta$ , the difference between the radiation frequency and the frequency of the impurity transition. Therefore, for an ensemble of impurities, the magnitude of the inhomogeneous broadening of the transition line is of great importance. The coherence relaxation time in the system, which in turn depends on the crystal temperature  $T$ , is also of significant importance. It is believed that the main mechanism of coherence relaxation is the interaction of the impurity center with lattice vibrations.

The spectrum of excited states of hydrogen-like donors in germanium is well described within the effective mass approximation, which gives a fourfold degeneracy of the excited states, while for the  $1s$  state the degeneracy is partially lifted by the central cell potential, and it splits off onto  $1s(A_1)$  singlet and  $1s(T_2)$  triplet. In Fig. 1b a diagram of arsenic donor levels in germanium is shown. The position of the ground state  $1s(A_1)$  is determined by the value of valley-orbital interaction, the so-called “chemical shift”. The mass anisotropy in the conduction band leads to the splitting of states with different values of the orbital and magnetic quantum numbers, which characterize the envelope of the wave function in the effective mass method the  $2s$ ,  $2p_0$ ,  $2p_{\pm}$  states have different binding energies. Among the traditionally used group-V donors, the most convenient from the point of view of research is arsenic, since having the largest chemical shift, approximately 4 meV, which, in the case of liquid helium temperature (4.2 K), makes it possible to minimize the thermal emission of charge carriers to the first excited level  $1s(T_2)$ , which is a factor in reducing the coherence time of excited dipoles at the transition between the ground state  $1s(A_1)$  and that excited state. In the present work, to create coherent superpositions, we used the  $1s(A_1) \rightarrow 2p_0$  transition in arsenic donors in germanium, as the most optimal in terms of limiting the thermal ionization of the upper level.

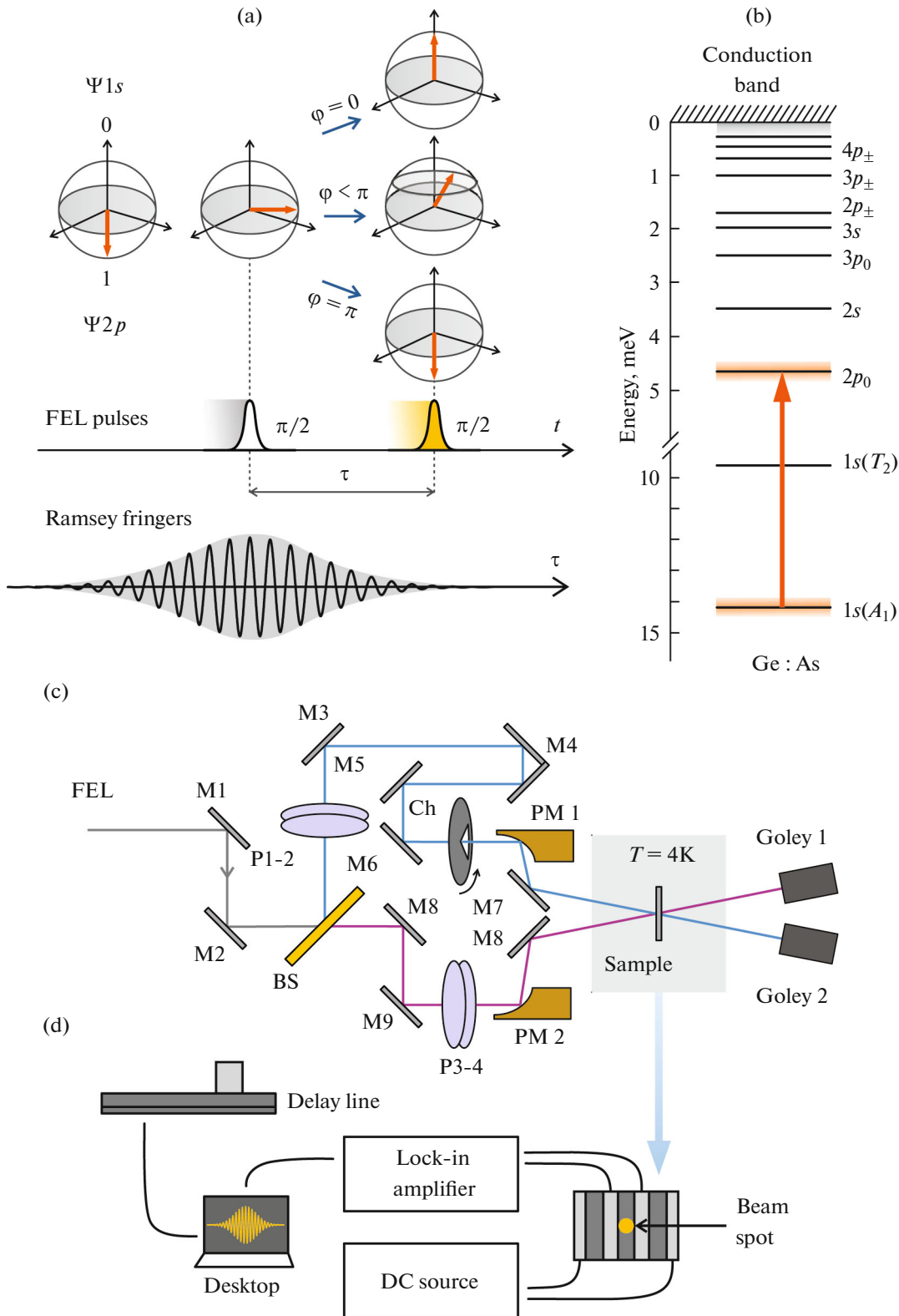


**Fig. 1.** Illustration of the impact of a pair of Ramsey pulses on the state of a two-level system (a). Scheme of As donor levels in Ge (b). The arrow shows the transition at which coherent superpositions are excited. Optical scheme of measurements of the Ramsey method. M1-10—mirrors, M4—moving mirror, BS—beam splitter, P1-4—polarizers, Ch—beam chopper, PM1,2—parabolic mirrors, FEL—free electron laser radiation (c). Electrical scheme of experiment (d).

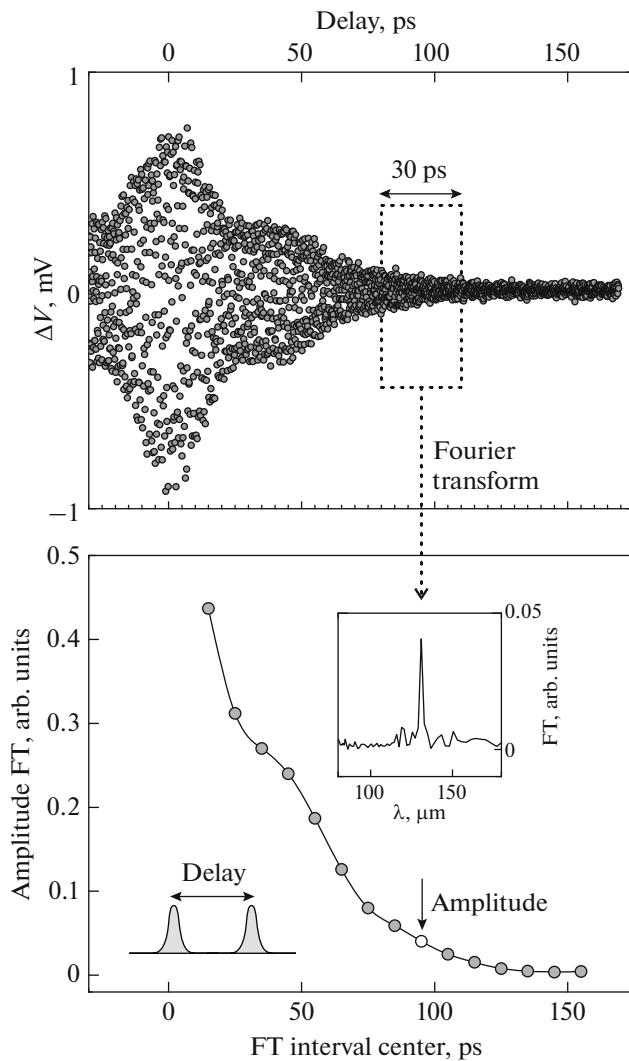


**Fig. 2.** Observation of Ramsey oscillations. Top—Ramsey fringes as a function of the delay time  $\tau$ , bottom—dependence of the amplitude of the spectral component on the central point of the 30 ps delay interval of the Fourier transform.

## EXPERIMENTAL

The NovoFEL setup at the Siberian Center for Synchrotron and Terahertz Radiation [11, 16], consisting of three free electron lasers (FELs), was used as a source. In this experiment we used a terahertz FEL with a tunable range of  $\lambda = 90\text{--}340\ \mu\text{m}$ , a pulse duration of  $\sim 100\ \text{ps}$ , and a repetition rate of 5.6 MHz. The characteristic FEL linewidth is about  $1\ \mu\text{m}$  (0.1 meV). The input radiation pulse was attenuated using a polarizer and divided into two parts, approximately equal in intensity, using a polypropylene beamsplitter. In accordance with the diagram (Fig. 1c), one of the pulses passed through a delay line equipped with a step motor, which allows varying the delay between pulses in automatic mode from  $\tau = -250$  to  $\tau = 500\ \text{ps}$  from zero path difference. Using a parabolic mirror, the

radiation was focused on the sample surface into a spot  $\sim 1\ \text{mm}$  in diameter. The radiation of both beams was modulated using a chopper at a frequency of 140 Hz, located in front of the entrance window of the cryostat with the sample. The average total power of the radiation incident on the sample did not exceed 10 mW. Basically, the experiment used the wavelength  $\lambda = 131.3\ \mu\text{m}$ , corresponding to the  $1s(A_1) \rightarrow 2p_0$  transition (9.44 meV), as well as  $\lambda = 160\ \mu\text{m}$  (7.7 meV) for comparison with nonresonant photoexcitation. Germanium crystals were grown by the Czochralski method with an arsenic concentration of  $5 \times 10^{13}\ \text{cm}^{-3}$ . The concentration of residual impurities, both donors and acceptors, did not exceed  $2 \times 10^{12}\ \text{cm}^{-3}$ . The sample had dimensions of  $0.5 \times 5 \times 10\ \text{mm}^3$ . The angle between polished faces  $5 \times 10\ \text{mm}^2$  was  $\sim 1.5^\circ$ . The sample was placed into Janis ST-100 liquid helium flow cryostat with TPX windows (transparent for wavelengths more than  $15\ \mu\text{m}$ ). Thermal contact and electrical isolation during mounting of the sample on a copper table was carried out by applying Apiezon N cryogenic paste to the rear surface of the sample.

Four Ti/Au contacts were deposited on the samples at 2 mm from each other. All measurements were carried out using a four-contact circuit. A current source was connected to the outer contacts and the value of the constant current was chosen in the range from 4 to 20  $\mu\text{A}$ . Under the influence of radiation, the conductivity of the central part changed, which led to the appearance of an alternating voltage signal, which was measured using inner contacts and fed to a lock-in amplifier with the possibility of subsequent recording and automatic construction of the signal value as a function of the position of delay line. The accumulation of the signal by the recording system was carried out after the stop of the mirror and a subsequent delay of 300 ms to improve the quality of the recorded signal. The recorded voltage drop between a pair of middle contacts turns out to be directly proportional to the population of the  $2p_0$  level, which is caused by the ejection of electrons into the conduction band due to both interaction with equilibrium phonons and secondary absorption of excitation quanta.

## RESULTS AND DISCUSSION

Figure 2 shows the dependence of the photocurrent on the delay time between pulses. The dependence represents damped oscillations at the frequency of the impurity transition. The experimental dependences obtained contain both the realization of the coherent effect of the interaction of radiation with coherent superpositions of the states of arsenic donors in germanium (Ramsey oscillations), and the signal that can be observed upon detection by any receiver and characterizes only the shape of the excitation pulses (auto-correlation function). This part of the signal can be due to various reasons, such as non-resonant absorp-

tion of radiation by residual impurities and arsenic donors in the presence of a population of excited levels due to thermal population. One of the features indicating the existence of the coherent effect is the delay of the response compared to the signal with the duration of the autocorrelation function, as well as the presence of the 131  $\mu\text{m}$  spectral line in this delayed signal part. The autocorrelation function was measured using another detector (for example, a Golay cell) or the sample itself using a wavelength that was not resonant for the investigated transition. Figure 2 shows the time delay dependence of the amplitude of the spectral component corresponding to the impurity transition frequency. Coherent superpositions continue to be observed when the signal is visually compared with the noise level. As follows from the experimental data, the shape of the signal envelope cannot be described as a simple exponentially decreasing function even for delays exceeding pulse duration.

### THEORETICAL MODEL

The theoretical description was based on a semiclassical model, in which the impurity atom was considered as a two-level quantum system, while the electromagnetic field (two successive pulses of electromagnetic radiation at a frequency close to the impurity transition frequency) was described classically. The rotating wave approximation was used. The Hamiltonian of the system, neglecting the interaction with lattice vibrations, has the form:

$$H = H_0 + \mu E_1(t) \cos(\nu t) + \mu E_2(t - \tau) \cos(\nu t + \varphi), \quad (1)$$

where  $H_0$  is the Hamiltonian of the unperturbed system,  $\mu$  is the dipole moment of transition,  $E_{1,2}(t)$  are the time-dependent amplitudes of the fields of two pulses of external radiation,  $\nu$  is the circular frequency of this radiation,  $\tau$  is the time delay between two pulses,  $\varphi$  is the phase difference of the radiation in the first and second pulses, determined by  $\tau$ .

If we neglect the relaxation of both population (longitudinal relaxation) and coherence (transverse relaxation), then it is convenient to construct a description of the interaction of an atom with a field in this case using the probability amplitude method [19], in which the wave function of the system can be expressed by the following superposition:

$$\Psi(t) = a_1(t) \varphi_1 e^{-i\omega_1 t} + a_2(t) \varphi_2 e^{-i\omega_2 t}, \quad (2)$$

where  $\varphi_1$  and  $\varphi_2$  are the wave functions of the atom unperturbed by the field (eigenfunctions of the operator  $H_0$ ),  $\omega_1$ ,  $\omega_2$  are the frequencies corresponding to the energies of the atomic levels. Substituting the wave function (2) into the Hamiltonian (1), after simple mathematical operations, one can obtain a system of equations for the probability amplitudes, which sets

the system dynamics under the action of a sequence of two resonant pulses of an electromagnetic field:

$$\begin{cases} a_1' = -\frac{i}{2} a_2 (\Omega_1(t) e^{i\delta t} + \Omega_2(t - \tau) e^{i(\delta t + \varphi)}) \\ a_2' = -\frac{i}{2} a_1 (\Omega_1(t) e^{-i\delta t} + \Omega_2(t - \tau) e^{-i(\delta t + \varphi)}), \end{cases} \quad (3)$$

where  $\Omega_1$  and  $\Omega_2$  are the time-dependent Rabi frequencies for the fields associated with the first and second pulses, respectively, and are given by:

$$\Omega_{1,2}(t) = \frac{\mu_{21} E_{1,2}(t)}{\hbar}, \quad (4)$$

where  $\mu_{21}$  is the transition matrix element,  $\delta$  is the detuning value. However, it is extremely difficult to consider the relaxation in the system with respect to the probability amplitudes. It is convenient to pass to the description of the system in terms of real quantities, such as the level populations and the real and imaginary parts of the dipole moment of the impurity center<sup>1</sup>.

$$\begin{cases} N' = -\Omega_1 R_2 - \Omega_2 T_2 - \gamma_l (1 + N) \\ R_2' = N (\Omega_1 + \Omega_2 \cos \varphi) + \delta R_1 - \gamma_t R_2 \\ T_2' = N (\Omega_1 \cos \varphi + \Omega_2) + \delta T_1 - \gamma_t T_2 \\ R_1' = N \Omega_2 \sin \varphi - \delta R_2 - \gamma_t R_1 \\ T_1' = -N \Omega_1 \sin \varphi - \delta T_2 - \gamma_t T_1. \end{cases} \quad (5)$$

Relaxation terms are additionally introduced into this system in the usual way, which determine the rates of longitudinal ( $\gamma_l$ ) and transverse ( $\gamma_t$ ) relaxation (population and coherence relaxation, respectively). The vectors  $N_1$ ,  $R_1$ ,  $R_2$ ,  $T_1$ ,  $T_2$  are expressed in terms of the probability amplitudes as follows:

$$\begin{aligned} N &= a_2 a_2^* - a_1 a_1^*, \\ R_1 &= a_1^* a_2 e^{i\delta t} + a_1 a_2^* e^{-i\delta t}, \\ iR_2 &= a_1^* a_2 e^{i\delta t} - a_1 a_2^* e^{-i\delta t}, \\ T_1 &= a_1^* a_2 e^{i(\delta t + \varphi)} + a_1 a_2^* e^{-i(\delta t + \varphi)}, \\ iT_2 &= a_1^* a_2 e^{i(\delta t + \varphi)} - a_1 a_2^* e^{-i(\delta t + \varphi)}, \end{aligned} \quad (6)$$

<sup>1</sup> It is also possible to solve the equations directly with respect to the elements of the density matrix, which is equivalent to the approach used in this work, however, the off-diagonal elements are rapidly oscillating functions, and the diagonal ones are smooth functions of time, which complicates the numerical calculation procedure. If we get rid of the rapidly oscillating part, reducing the system to real parameters that characterize the population of the states and the amplitude of the dipole moment, then in the presence of an arbitrary relative phase shift of the field oscillations in two excitation pulses, the system cannot be strictly reduced to three real parameters (Bloch vectors), and we need to introduce more two parameters that take into account the phase shift.

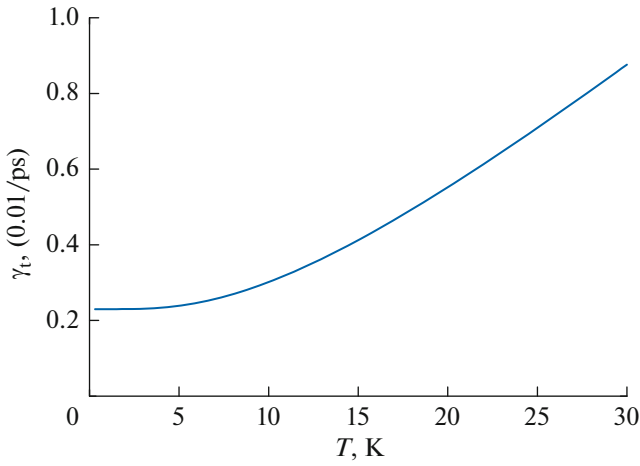


**Fig. 3.** Calculated dependence of the transverse relaxation rate  $\gamma_t$  upon excitation of coherent superpositions of arsenic donor states in germanium at the  $1s(A_1) \rightarrow 2p_0$  transition on the crystal lattice temperature ( $T$ ).

i.e.,  $N$  is the difference between the populations of the upper and lower levels, and the values  $R_1$ ,  $R_2$ ,  $T_1$ ,  $T_2$  characterize the dipole moment excited by a sequence of two excitation pulses shifted in phase relative to each other. System (6) is like the equations for the Bloch vectors [19] and in the case of two excitation pulses with different phases, the system can be governed by five equations for clarity or reduced to three equations. The population of the upper level of a two-level atom ( $N_2$ ) depends on time, the detuning of the transition frequency from the frequency of the exciting radiation and on the phase difference of the radiation in the first and second excitation pulses, determined by the delay time ( $\tau$ ) between pulses ( $\varphi = (\omega_2 - \omega_1)\tau$ ), and is found as follows:

$$N_2(t, \delta, \varphi) = \frac{1}{2}(1 + N). \quad (7)$$

Ramsey fringes were observed experimentally by recording the current ( $J$ ) due to the photothermal ejection of carriers from the upper excited level of the donor center into the conduction band. Thus, the electric current, which depends on the time delay between the pump pulses, is proportional to the population of the upper level of a shallow donor, averaged over the observation time and over the frequencies of impurity transitions associated with inhomogeneous broadening in the system. It was assumed that the frequencies obey the normal distribution law with a dispersion corresponding to the width of the impurity transition line.

$$J(\tau) \sim \iint N_2(t, \delta, \Delta\omega\tau) \frac{1}{\sqrt{2\pi\sigma}} e^{-\frac{(\delta-\Delta)^2}{2\sigma^2}} d\delta dt. \quad (8)$$

The damping of the coherent part is caused by two factors, one of which is the relaxation of coherence in

the system (transverse relaxation), the other is the desynchronization of dipoles oscillations formed by donor centers in coherent superpositions of states due to the inhomogeneous broadening of the lines of impurity transitions. To estimate the rate of coherence relaxation, it is assumed that its main mechanism is associated with the interaction of excited donors with lattice vibrations. An important part while modeling various coherent effects is the estimation of the population relaxation rates ( $\gamma_i$ ) and coherence ( $\gamma_t$ ) in the system. It is assumed that the main mechanism of both longitudinal and transverse relaxation is the interaction with phonons. However, the interaction with phonons also causes thermal transitions between the levels of impurity centers without changing the population of states averaged over the ensemble of donors but leading to a loss of coherence. The coherence relaxation rate was estimated using the following expression:

$$\gamma_t = \sum_i \gamma_{\downarrow i} (n_i(T, E_i) + 1) + \sum_j \gamma_{\uparrow j} n_j(T, E_j), \quad (9)$$

where  $\gamma_{\downarrow i}$ ,  $\gamma_{\uparrow j}$  are the rates of various spontaneous transitions during interaction with phonons, numbered by indexes  $i$  and  $j$ , down (phonon emission) and up (phonon absorption) in energy, respectively;  $n_{i,j}(T, E_{i,j})$  are the lattice temperature ( $T$ ) dependent occupation numbers of phonons with energies  $E_i$  and  $E_j$  corresponding to the energies of the  $i$  and  $j$  transitions. The summation over  $i$  and  $j$  includes transitions from both the upper  $2p$  and lower  $1s$  states, which form superposition (2). In Ge:As, the energy gap between the ground state and the first excited state  $1s(T_2)$  is 4.24 meV, and thermal transitions also occur between these states (the  $1s(T_2)$  state has a noticeable population at temperatures above 10 K) without changing the average population, but also destroying coherence.

Using the rates of spontaneous transitions calculated in [20, 21] and taking into account the experimental data on the lifetimes of excited states of Sb and As donors in germanium [11, 16], we can estimate the coherence loss rate by formula (9), which gives higher values of coherence relaxation rates in comparison with the longitudinal relaxation rate  $\gamma_1$ . The temperature dependence of  $\gamma_t$ , assuming that the occupation numbers obey the Bose–Einstein statistics, in the case of excitation of coherent superpositions at the  $1s(A_1) \rightarrow 2p_0$  transition in Ge:As, is shown in Fig. 3. It can be seen from the calculations that the coherence relaxation rate has strong temperature dependence. Therefore, when implementing an experiment on observing Ramsey oscillations in germanium, it is necessary to ensure proper temperature conditions of the sample under optical excitation. The lower limit of the coherence loss rate is related to the spontaneous decay of the excited state via emission of intravalley acoustic phonons and coincides with the lower limit of

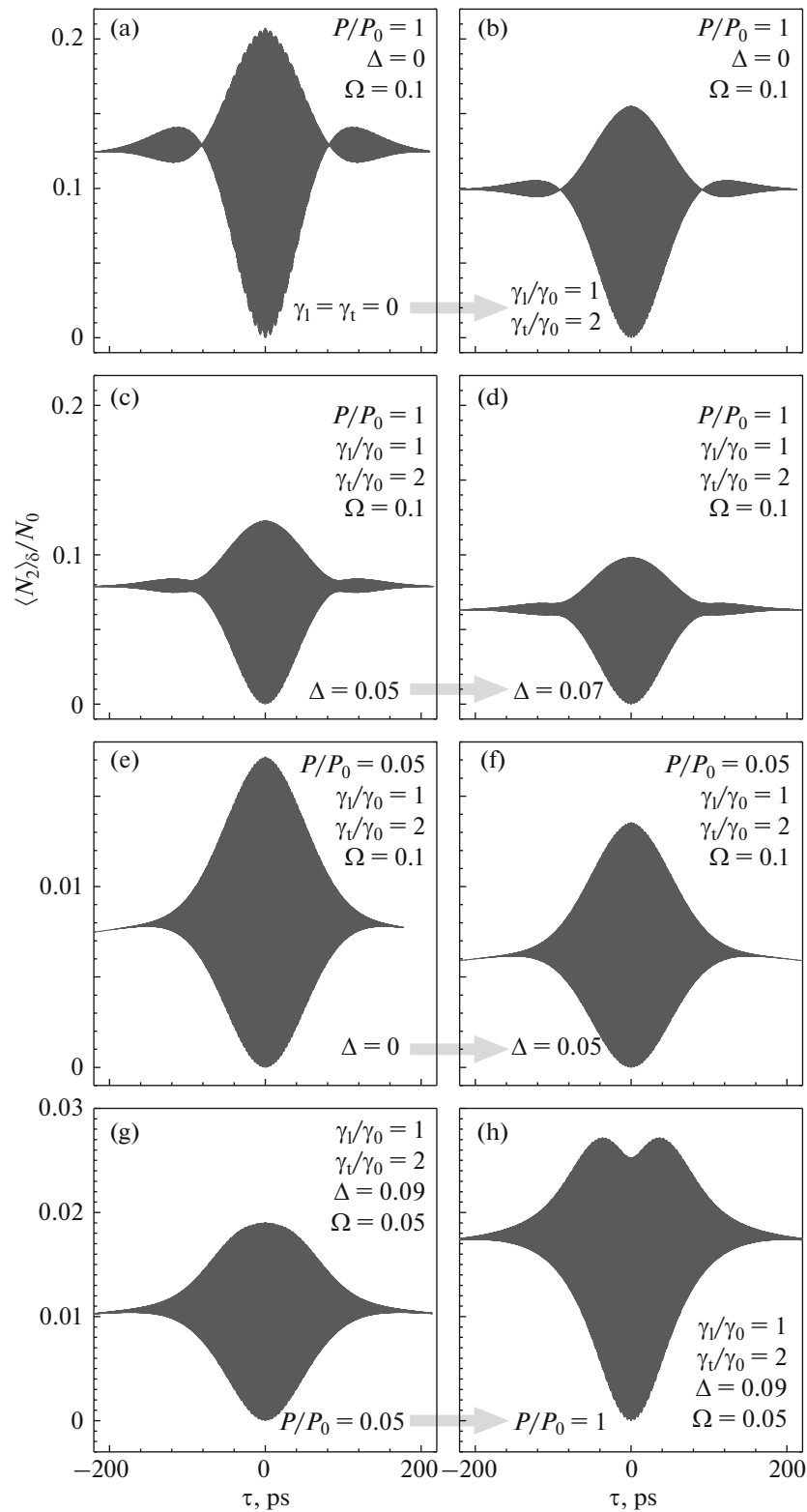


**Fig. 4.** Theoretical dependences of the population of the upper level of the excited transition on the delay time  $\tau$ , considering the relaxation of population and coherence in the system. Parameter designations in the figures:  $\Delta$  is the detuning of the excitation line from the center of the impurity line,  $\Omega$  is the value of the inhomogeneous broadening of the impurity line,  $(\gamma_l)$  and  $(\gamma_t)$  are the rates of longitudinal and transverse relaxation, respectively (population and coherence relaxation),  $P$  is the power of the exciting radiation pulse,  $P_0$  is the radiation power corresponding to the  $\pi/2$  pulse;  $\gamma_0 = 0.125 \text{ ns}^{-1}$  is the experimental value for  $\gamma_l$ .

the longitudinal relaxation rate. Thus, at liquid helium temperature, the coherence loss time, according to theoretical estimates, is  $\sim 450$  ps. At a temperature of about 20 K (estimated to this temperature, heating can occur under experimental conditions [11]), the coherence relaxation time drops to approximately 170 ps.

The damping of Ramsey fringes associated with inhomogeneous broadening is a more complex problem that requires numerical simulation in a rigorous approach, since the shape of the envelope of the received signal can be quite non-trivial. Figure 4 shows the theoretical dependences of the population of the upper level of the excited transition on the delay time between excitation pulses for various parameters. In particular Fig. 4a shows dependences without taking into account relaxation processes.

It can be seen from Figs. 4a, 4b that for certain parameters and certain values of the delay time between pulses, the oscillation amplitude vanishes. This behavior is typical when a large number of harmonics with close frequencies are summed, which, in fact, occurs when observing Ramsey fringes<sup>2</sup>. As the inhomogeneous broadening of the impurity line ( $\Omega$ ) decreases, the vanishing point disappears, which is caused by an insufficiently large frequency distribution of harmonics (dipole moments associated with excited donors) to provide such dynamics. The same trend is also observed with the decrease of excitation pulses power. This is due to the fact that, at a low power, impurities with a transition frequency located at the edge of the impurity absorption line are excited weakly and practically do not contribute to the observed signal, which is equivalent to a decrease in the linewidth of the impurity transition line. At a sufficiently high value of the pulse power (close to  $\pi/2$ ) there is an asymmetry with respect to the horizontal axis, which disappears while decreasing the excitation power. The combined effect of relaxation in the system and detuning of the excitation line from the center of the impurity line  $\Delta$  (Figs. 4c, 4d) is more complex resulting in appearance of local minimum of Ramsey fringes. Note that neither relaxation nor detuning lead to such an effect. However, sufficiently large detuning values (approaching in value to the width of the transition line) at a sufficient excitation power (close to  $\pi/2$ ) appear as a “trough” at a zero value of the delay time.

Evidently, it is rather difficult to obtain the entire variety of Ramsey oscillation envelope shapes in an experiment due to the criticality of the temperature regime, which requires the use of low values of the excitation pulse power.

<sup>2</sup> The vanishing point of the oscillation amplitude (and its presence) depends on the frequency distribution of the amplitudes of these harmonics (in the general case, it does not obey the normal distribution law), as well as on the relaxation rate.

## CONCLUSIONS

The possibility of observing Ramsey fringes upon excitation of the  $2p_0$  state of an arsenic donor in germanium by pulsed terahertz radiation at cryogenic temperatures has been experimentally shown. Registration of fringes in the population of the  $2p_0$  state was carried out due to the presence of a thermal ejection of electrons into the conduction band, which can be considered as a demonstration of incoherent readout of a coherent state. The simulations taking into account the times of longitudinal and transverse relaxation show that the observed shape of the envelope of Ramsey fringes depends on the width of the impurity transition line, the detuning from resonance, and the excitation intensity.

## ACKNOWLEDGMENTS

The authors are grateful for the participation of the operators of the NovoFEL free electron laser. The measurements were performed at the Shared-Use Resource Center “Siberian Synchrotron and Terahertz Radiation Center” of the Novosibirsk FEL facility at Budker Institute of Nuclear Physics, Siberian Branch, Russian Academy of Sciences.

## FUNDING

This work was supported by Russian Science Foundation (project no. 19-72-20163).

## CONFLICT OF INTEREST

The authors declare that they have no conflicts of interest.

## REFERENCES

1. Curtolo, D.C., Friedric, S., and Friedrich, B., *J. Cryst. Process Technol.*, 2017, vol. 7, no. 4, p. 65.
2. Tyryshkin, A.M., Tojo, S., Morton, J.J., et al., *Nat. Mater.*, 2012, vol. 11, no. 2, p. 143.
3. Fuechsle, M., Miwa, J.A., Mahapatra, S., Ryu, H., Lee, S., Warschkow, O., Hollenberg, L.C.L., Klimeck, G., and Simmons, M.Y., *Nat. Nanotech.*, 2012, vol. 7, no. 4, p. 242.
4. Struck, T., Hollmann, A., Schauer, F., et al., *NPJ Quantum Inf.*, 2020, vol. 6, p. 40.
5. Zinovieva, A.F., Dvurechenskii, A.V., Stepina, N.P., et al., *Phys. Rev. B*, 2020, vol. 81, no. 11, p. 113303.
6. Lawrie, W.I.L., Hendrickx, N.W., van Riggelen, F., et al., *Nano Lett.*, 2020, vol. 20, no. 10, p. 7237.
7. Litvinenko, K.L., Bowyer, E.T., Greenland, P.T., Stavrias, N., Li, J., Gwilliam, R., Villis, B.J., Matmon, G., Pang, M.L.Y., Redlich, B., van der Meer, A.F.G., Pidgeon, C.R., Aeppli, G., and Murdin, B.N., *Nature*, 2015, vol. 6, p. 6549.
8. Meirzada, I., Wolf, S.A., Naiman, A., Levy, U., and Bar-Gill, N., *Phys. Rev. B*, 2019, vol. 100, no. 12, p. 125436.



9. Kane, B.E., in *2000 Scalable Quantum Computers*, Braunstein, S.L., Lo, H.K., and Kok, P., Eds., Berlin: Wiley, 2000, p. 253.
10. Clauws, P., Broeckx, J., Rotsaert, E., and Vennik, J., *Phys. Rev. B*, 1988, vol. 38, no. 17, p. 12377.
11. Zhukavin, R.Kh., Kovalevskii, K.A., Choporova, Yu.Yu., Tsyplenkov, V.V., Gerasimov, V.V., Bushuikin, P.A., Knyazev, B.A., Abrosimov, N.V., Pavlov, S.G., Hübers, H.-W., and Shastin, V.N., *JETP Lett.*, 2019, vol. 110, no. 10, p. 677.
12. Itoh, K.M., Haller, E.E., Hansen, W.L., et al., *Appl. Phys. Lett.*, 1994, vol. 64, no. 16, p. 2121.
13. Bachmann, D., Rosch, M., Suess, M.J., Beck, M., Unterrainer, K., Darmo, J., Faist, J., and Scalari, G., *Optica*, 2016, vol. 3, no. 10, p. 1087.
14. Muravjov, A.V., Strijbos, R.C., Fredricksen, C.J., Weidner, H., Trimble, W., Withers, S.H., Pavlov, S.G., Shastin, V.N., and Peale, R.E., *Appl. Phys. Lett.*, 1998, vol. 73, p. 3037.
15. Greenland, P.T., Matmon, G., Willis, B.J., et al., *Phys. Rev. B*, 2015, vol. 92, no. 16, p. 165310.
16. Zhukavin, R.Kh., Kovalevskii, K.A., Sergeev, S.M., Choporova, Yu.Yu., Gerasimov, V.V., Tsyplenkov, V.V., Knyazev, B.A., Abrosimov, N.V., Pavlov, S.G., Shastin, V.N., Schneider, H., Deßmann, N., Shevchenko, O.A., Vinokurov, N.A., Kulipanov, G.N., and Hübers, H.-W., *JETP Lett.*, 2017, vol. 106, no. 9, p. 571.
17. Zhukavin, R.Kh., Bushuikin, P.A., Kukotenko, V.V., Choporova, Yu.Yu., Deßmann, N., Kovalevsky, K.A., Tsyplenkov, V.V., Gerasimov, V.V., Knyazev, B.A., Abrosimov, N.V., and Shastin, V.N., *JETP Lett.*, 2022, vol. 116, p. 137.
18. Ramsey, N.F., *Rev. Mod. Phys.*, 1990, vol. 62, no. 3, p. 541.
19. Scully, M.O. and Zubairy, M.S., *Quantum Optics*, Cambridge: Cambridge Univ. Press, 1999.
20. Tsyplenkov, V.V. and Shastin, V.N., *Semiconductors*, 2018, vol. 52, no. 12, p. 1573.
21. Tsyplenkov, V.V. and Shastin, V.N., *Semiconductors*, 2019, vol. 53, no. 10, p. 1334.